HHS Public Access

Author manuscript

Cell Metab. Author manuscript; available in PMC 2017 September 13.

Published in final edited form as:

Cell Metab. 2016 September 13; 24(3): 420–433. doi:10.1016/j.cmet.2016.08.005.

Connexin 43 Mediates White Adipose Tissue Beiging by Facilitating the Propagation of Sympathetic Neuronal Signals

Yi Zhu[1,2], **Yong Gao**[3,4], **Caroline Tao**[1], **Mengle Shao**[1], **Shangang Zhao**[1], **Wei Huang**[5], **Ting Yao**[3,6], **Joshua A. Johnson**[1], **Tiemin Liu**[3], **Aaron M. Cypess**[7], **Olga Gupta**[1], **William L. Holland**[1], **Rana K. Gupta**[1], **David C. Spray**[8], **Herbert B. Tanowitz**[9], **Lei Cao**[5], **Matthew D. Lynes**[10], **Yu-Hua Tseng**[10], **Joel K. Elmquist**[3], **Kevin W. Williams**[3], **Hua V. Lin**[2], and **Philipp E. Scherer**[1,*]

[1]Touchstone Diabetes Center, Department of Internal Medicine, University of Texas Southwestern Medical Center, Dallas, Texas 75390, USA

[2]Lilly Research Laboratories, Division of Eli Lilly and Company, Indianapolis, Indiana 46285, USA

[3]Division of Hypothalamic Research, Department of Internal Medicine, The University of Texas Southwestern Medical Center at Dallas, Dallas, TX 75390, USA

[4]National Laboratory of Medical Molecular Biology, Institute of Basic Medical Science, Chinese Academy of Medical Science and Peking Union Medical College, Beijing 100005, P.R. China

[5]Department of Cancer Biology and Genetics, College of Medicine, The Ohio State University, Columbus, Ohio, 43210, USA

[6]Department of Physiology and Pathophysiology, Xi'an Jiaotong University School of Medicine, 76 West Yanta Road, Xi'an, Shaanxi 710061, People's Republic of China

[7]Translational Physiology Section, Diabetes, Endocrinology, and Obesity Branch, National Institute of Diabetes and Digestive and Kidney Diseases, NIH, Bethesda, MD 20892, USA

[8]Departments of Neuroscience and Medicine (Cardiology), Albert Einstein College of Medicine, Bronx, NY 10461, USA

[*]Correspondence: philipp.scherer@utsouthwestern.edu.

ACCESSION NUMBERS

The accession number for the microarray data reported in this paper is GEO: GSE84860.

SUPPLEMENTAL INFORMATION

Supplemental Information includes supplemental experimental procedures, four figures, and one table.

AUTHOR CONTRIBUTIONS

Y.Z. conceived, designed, performed most of the experiments and analyzed the data. Y.G, T.Y, and T.L. provided POMC Xbp1s mice, performed lucifer yellow dye coupling experiment and analyzed the data. C.T. performed the denervation experiments. W.H. made the Connexin 43 adeno-associated virus. O.G. provided human omental adipose tissue slides. A.M.C., M.D.L. and Y.-H.T. provided human deep neck adipose tissue slides and analyzed GJA1 gene expression between human subcutaneous and deep neck adipose tissues. P.E.S. conceived, designed, and supervised the project. Y.Z. and P.E.S. wrote the manuscript. M.S., S.Z., J.J., A.M.C., O.G., W.L.H., R.K.G., D.C.S., H.B.T., L.C., Y.-H.T., J.K.E., K.W.W. and H.V.L. provided expertise and feedback on the manuscript.

Conflict of interest: none.

[9]Departments of Pathology and Medicine, Albert Einstein College of Medicine, Bronx, NY 10461, USA

[10]Joslin Diabetes Center, Harvard Medical School, Boston, MA 02215, USA

Abstract

"Beige" adipocytes reside in white adipose tissue (WAT) and dissipate energy as heat. Several studies have shown that cold temperature can activate proopiomelanocortin-expressing (POMC) neurons and increase sympathetic neuronal tone to regulate WAT beiging. However, WAT is traditionally known to be sparsely innervated. Details regarding the neuronal innervation and more importantly, the propagation of the signal within the population of "beige" adipocytes are sparse. Here, we demonstrate that beige adipocytes display an increased cell-to-cell coupling via connexin 43 (Cx43) gap junction channels. Blocking of Cx43 channels by 18α-glycyrrhetinic acid decreases POMC activation-induced adipose tissue beiging. Adipocyte-specific deletion of Cx43 reduces WAT beiging to a level similar to that observed in denervated fat pads. In contrast, overexpression of Cx43 is sufficient to promote beiging even with mild cold stimuli. These data reveal the importance of cell-to-cell communication in adipose tissue for the propagation of limited neuronal inputs, resulting in effective beiging.

eTOC Blurb

Cold activates the "beiging" of white adipocytes through a sympathetic neuronal signal. However, white adipose tissue is sparsely innervated. Here, XXX et al show that connexin 43 (Cx43) cell-to-cell gap junction channels are necessary for the propagation of sympathetic signals leading to the beiging of white adipocyte clusters.

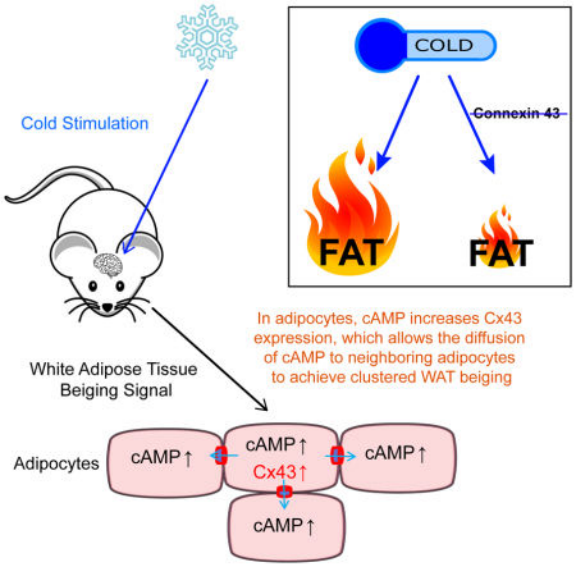

Introduction

When energy intake exceeds energy expenditure, excess calories are stored in the adipose tissue (Spiegelman and Flier, 2001). There are at least two distinct types of adipose tissues,

white (WAT) and brown (BAT), with WAT primarily storing energy as triglycerides in lipid droplets and BAT mediating adaptive thermogenesis and dissipating chemical energy as heat. These depots play opposite roles in energy metabolism. Dysfunctional WAT accumulates in most individuals upon excess caloric intake, resulting in obesity and an enhanced predisposition to many pathophysiological changes, including diabetes, cardiovascular disease and cancer. In contrast, BAT is dramatically reduced within the first few months after birth. However, in the past few years, a higher appreciation has emerged for the fact that even humans have the ability to induce a third type of adipocyte - the "beige" or "brite" adipocyte - in specific WAT depots, with a distinct and different origin and molecular identity from classical brown adipocytes (Petrovic et al., 2010; Wang et al., 2013; Wu et al., 2012).

PET scanning reveals substantial depots of UCP1 expressing brown-like fat, particularly in the supraspinal, supraclavicular, pericardial and neck regions of adult humans (Cypess et al., 2009; van Marken Lichtenbelt et al., 2009; Virtanen et al., 2009). Cold is the major physiological factor that induces the emergence of beige/brite adipocytes in WAT, but multiple peripheral factors and secreted molecules have also been identified and shown to modulate the development of beige patches in WAT (Bartelt and Heeren, 2014; Wu et al., 2013). Centrally, specific neuronal populations, including agouti-related protein (AgRP) neurons and proopiomelanocortin (POMC) neurons in the arcuate region of the hypothalamus, have been implicated in controlling WAT beiging (Dodd et al., 2015; Ruan et al., 2014; Williams et al., 2014). Coinfusion of insulin and leptin activates POMC neurons and leads to an increase in WAT beiging (Dodd et al., 2015). In contrast, fasting and chemical or genetic activation of AgRP neurons suppresses the beiging of WAT (Ruan et al., 2014). However, compared to BAT, WAT is not well innervated (Murano et al., 2009); Zeng and colleagues estimated that only 8% ± 4.6% of adipocytes are in direct contact with sympathetic neuronal termini (Zeng et al., 2015). The mechanism by which the neuronal fibers control a cluster of beige adipocytes in WAT remains to be further explored.

Direct cell-to-cell contact is a possible form of local signaling for eukaryotic cells. Animal cells contain gap junctions that connect across the intercellular space and allow for signaling factors in the cytosol to easily pass between cells that are connected by this mechanism. A gap junction channel is composed of two connexons (or hemichannels), each composed of homo- or hetero-hexamers of connexin protein subunits. Different connexin channels have different structural stability (Stout et al., 2015) and conductivities; generally, these channels have a molecular weight cutoff of approximately 1 kDa, big enough to allow the passing of many ions, cAMP and other small molecules and metabolites (Weber et al., 2004). Thus far, 21 human genes and 20 mouse genes for connexins have been identified. Each connexin shows tissue- or cell type-specific expression, and most organs and many cell types express more than one connexin. Several reports describe that gap junction function is tightly modulated during WAT and BAT development (Schneider-Picard et al., 1980; Yanagiya et al., 2007). Adipocytes in BAT of adult mice seem functionally connected via gap junctions, whereas adipocytes in WAT appear to be connected much less effectively (Burke et al., 2014).

Using a lucifer yellow (LY) dye-based coupling approach to gauge intercellular communication, we find that cold-induced beige adipocytes are coupled at a much higher percentage compared to white adipocytes, and this coupling is specifically mediated by Cx43 channels. Our groups have previously shown that the inducible activation of Xbp1s in POMC neurons results in enhanced sympathetic outflow, resulting in acutely increased beiging. Here, we show that blocking Cx43 channels with a chemical inhibitor, such as 18α-glycyrrhetinic acid (AGA), greatly reduced WAT beiging induced by POMC neuron - specific Xbp1s overexpression. A UCP1 promoter driven inducible Cx43 gene deletion also reduced cold-induced WAT beiging to levels similar to those observed in chemically denervated WAT. In contrast, AAV-mediated Cx43 expression in adipose tissue promotes WAT beiging in mice individually housed, even at room temperature. When *in vitro* differentiated adipocytes were treated with 8-bromo-cAMP, a cell membrane permeable analog of cAMP, increased Cx43 expression is noted. Based on these observations, we postulate that sympathetic nerves activate adipocytes they innervate via synapses, leading to an increase in intracellular cAMP. This in turn increases and activates Cx43 gap junction channels, allowing efficient propagation of sympathetic signals to surrounding cells in WAT, thereby allowing the activation of entire clusters of beige adipocytes through innervation of a single cell. Since Cx43 expression is reduced in obesity and aging, upregulating Cx43 may be a viable strategy to overcome the reduced beiging under these conditions and thereby improve metabolic function.

Results

Increased Gap Junction Activity and Cx43 Expression during WAT Beiging

Sympathetic stimulation has long been recognized to mobilize fatty acids from adipose tissues (Dalziel, 1989). However, WAT is sparsely innervated compared to BAT. Cinti and colleagues demonstrated that tyrosine hydroxylase positive nerve fibers (indicative of noradrenergic fibers) increased after cold acclimatization in adipose tissue, but the penetrance is still too low for neural fibers to reach every adipocyte within the fat pad (Murano et al., 2009). Given the prominent clustering pattern of beige adipocytes in WAT, we decided to determine whether those beige adipocytes were interconnected. A gap junction permeable dye (LY) was injected into unilocular adipocytes in mice housed at thermoneutrality (30°C). This revealed very rare occurrences of diffusion (Fig. 1A, left panel). In contrast, LY injected into adipocytes from mice housed at 6°C with multilocular lipid droplets in WAT (typical characteristics of beige adipocytes) diffused to an average of 1.75 surrounding cells (Fig. 1A, right panel), suggesting increased gap junction connectivity in beige adipocytes compared to white adipocytes.

To investigate genes responsible for increased gap junction connectivity, we performed a microarray study to compare gene expression of fat pads from mice housed in the cold (6°C) versus fat pads from mice housed at thermoneutrality (30°C). Ingenuity pathway analysis revealed an upregulation of pathways related to mitochondrial dysfunction, oxidative phosphorylation, TCA cycle and glycolysis, confirming the functional effects of the cold temperature on WAT (Fig. 1B). WAT beiging signature genes (UCP1, PGC1-α, and multiple mitochondrial genes) were also upregulated (Suppl. Table 1). There was a 2.90 fold increase

of Gja1, the gene encoding the Cx43 protein. No other connexin genes were detected by the same microarray experiment (Suppl. Table 1).

These data agree with previous studies that identified Cx43 as the most abundant connexin gene in the adipose tissue (Burke et al., 2014). Using qPCR assays, we verified that cold induces Cx43 gene expression 15-fold, a much higher *de facto* increase than the 2.90-fold change indicated by our microarray study. The β3 agonist CL316,243 also increased Cx43 expression by 5-fold (Fig. 1C). There was no effect of cold exposure or CL compound treatment on expression of other connexin genes, such as Cx26, Cx30.2, Cx32, Cx36 or Cx47, all of which are much less abundantly expressed and unaltered in terms of their levels compared to Cx43 (Fig. 1C).

UCP-1 Promoter Driven Cx43 Deletion Does Not Affect BAT Physiology and Thermal Adaptation to the Cold

To test the role of Cx43 in cold adaptation and BAT physiology, we generated a compound transgenic mouse model that is heterozygous for UCP1-rtTA and tetO responsive element (TRE)-Cre and homozygous for Cx43 flox alleles. Cx43 is deleted in UCP1 positive cells upon doxycycline (DOX) supplementation (Fig. 2A). The UCP1 promoter has the strongest activity in BAT, so we first investigated how the deletion of Cx43 affected the BAT morphology and function. 3 weeks after DOX supplementation in the diet (600mg/kg), there is a comparable 30%–40% decrease in Cx43 transcripts in either Cx43-KO BAT whole tissue lysates or isolated BAT adipocytes (Suppl. Fig. 1A). BAT has a dense vasculature that displays very high levels of Cx43 expression. Therefore, Cx43 expression levels from lysed preparations of BAT not only represent the Cx43 expression levels in the brown adipocytes *per se,* but reflect Cx43 protein expression in many different cell types within BAT. The higher resolution obtained with immunofluorescence staining reveals a much more robust deletion of Cx43 in BAT (Fig. 2B and 2C). There was no difference in body weight or glucose tolerance in Cx43-KO mice after 3 weeks of DOX supplementation on normal chow (Suppl. Fig. 1B and 1C). Despite the robust Cx43 reduction in Cx43-KO BAT, there were no distinguishable differences in morphology revealed by Trichrome staining (Fig. 2D) or H&E staining (Suppl. Fig. 1D).

One prominent function of BAT is thermal regulation during cold stress (Cannon and Nedergaard, 2004). UCP1 knockout mice or mice with dysfunctional BAT are cold intolerant (Enerback et al., 1997). In an acute cold tolerance test, both control and Cx43 KO mice started with body temperatures close to 37°C. Upon 4 hours housing at 6°C in the absence of food, body temperatures of both groups dropped comparably by 5°C (Fig. 2E). During acute short-term cold exposure, it is mainly muscle shivering that contributes to heat production (Cannon and Nedergaard, 2004). However, during prolonged (1 week and 3 weeks) cold exposure, a state during which heat generation heavily relies on functional BAT, body temperature also dropped to a similar extent independent of the presence or absence of Cx43 (Fig. 2H). During this 3-week time course, both groups gained a similar amount of body mass (Fig. 2I). At the end of 3 weeks of cold exposure, the same group of mice were switched back to room temperature for 2 hours to recover to normal body temperature, and then were exposed to cold again to repeat the acute cold tolerance test. With “pre-activated”

BAT, Cx43 KO mice behaved identically (Fig. 2F). Histological analysis of Cx43-KO mice post-chronic cold exposure did not show any differences in adipose tissue histology from control mice (Fig. 2G and Suppl. Fig. 1E). Combined, all these assays suggest that Cx43 KO mice have a normal BAT function.

UCP1 Promoter Driven Cx43 Deletion Blunts Cold Induced Metabolic Improvement

Beige adipocytes also have abundant UCP1 protein in their mitochondria when compared to mitochondria from BAT (Kazak et al., 2015), suggesting a strong UCP1 promoter activity in beige adipocytes. Indeed, UCP1 is highly induced in subcutaneous WAT (sWAT) after 48-hour cold exposure (due to the widespread increase in beige adipocytes) (Fig. 3A). As a consequence, CRE recombinase expression driven by UCP1-rtTA is also highly induced by the cold in the presence of doxycycline (Fig. 3B). As a consequence, our mouse model should also display a deletion of Cx43 in beige cells, especially after cold exposure. This is supported by the observed reduction of Cx43 levels in WAT after cold exposure (Fig. 3C, Suppl. Fig. 2A). Importantly, this is further corroborated by the significantly reduced coupling of beige adipocytes in response to the DOX treatment (Fig. 3D, Suppl. Fig. 2B). The deletion of Cx43 in beige adipocytes reduces cold-induced WAT beiging as judged by Trichrome staining (Fig. 3E), and by a reduction of signature genes for beiging (Fig. 3C).

Cold exposure has been shown to be a powerful way to improve glucose homeostasis in obese mice, and it is postulated that these metabolic improvements are partially driven via the activation of beige adipocytes under these conditions. Deletion of Cx43 and the reduction in sWAT beiging indeed blunts this improvement (Fig. 3F). Overall, cold-induced sWAT beiging is reduced in obese mice that were fed 12 weeks high-fat diet (HFD) prior to the cold exposure (Fig. 3C and 3G), and deletion of Cx43 further dampens this process (Fig. 3G). The only moderate increase in sWAT beiging under these HFD conditions in the presence of Cx43 may explain why abolishing Cx43 expression in those beige adipocytes did not result in a substantial change in overall GTT responses (Fig. 3F). However, the same data could form the basis for the argument that a more significiant improvement in glucose homeostatis could be achieved if more beige adipocytes were activated in obese mice. The deletion of Cx43 in beige adipocytes led to the accumulation of hepatic lipid droplets (Fig. 3G), increased levels of hepatic triglycerides (Suppl. Fig. 2C), an increase in circulating cholesterol and a trend towards increased circulating high density lipoprotein (Fig. 3H). Thus, these data demonstrate an essential role of Cx43 in cold-induced WAT beiging and the associated improvements of glucose and lipid homeostasis.

UCP1-Driven Cx43 Deletion and Adipose Tissue Denervation Impaired WAT Beiging to a Similar Level

Fat pads are innervated by sympathetic fibers, and cold-induced WAT lipolysis and beiging is driven at least partially via activation of sympathetic nerves (Dodd et al., 2015; Rosen and Spiegelman, 2006). Denervation has been shown to reduce lipolysis, WAT beiging, and increases the fat pad weight (Dodd et al., 2015). To determine whether Cx43-mediated WAT beiging is downstream of the sympathetic neuronal signaling, an experimental design was employed wherein unilateral denervation of WAT with sham procedure on the collateral side was implemented; after 2 weeks recovery from surgery, the mice were exposed to the cold

for one more week (Fig. 4A). Fat pad weights increased by 25.3% after denervation in control mice. Cx43 KO mice have approximately a 10.5% increase of weight in sham-operated fat pad when compared to control mice (no statistical significance), denervation failed to increase the fat pad weights in Cx43 KO mice (Fig. 4B). Denervated inguinal fat pad weights normalized to the sham fat pad weight in the same mouse was 25.3% in wildtype mice, compared to the 4.6% in Cx43 KO mice. Denervation greatly reduced cold-induced WAT beiging in control mice (Fig. 4C and 4D), and as expected, Cx43 KO mice had reduced WAT beiging in the sham fat pad. There was no further significant reduction in WAT beiging with the combination of Cx43 deletion and denervation (Fig. 4C and 4D). A similar pattern was also observed in beiging signature genes (Fig. 4E). In summary, UCP1-driven Cx43 deletion and denervation impaired WAT beiging to similar degrees.

Blocking of Cx43 Channels by 18α-Glycyrrhetinic acid (AGA) Inhibits Sympathetic Activation Induced WAT Beiging

Deletion of Cx43 in beige adipocytes in our mouse model relies on the cold-activation of the UCP1 promoter; however, after deletion of Cx43, WAT beiging is reduced and so is the UCP1 expression, potentially confounding the interpretation of results obtained for studying the role of Cx43 in beige adipocytes. To address this with a pharmacological rather than a genetic approach, we utilized the Cx43 channel blocker 18-α-glycyrrhetinic acid (AGA) and our previously published “brain beiging” model, which activates sympathetic signals by doxycycline-induced expression of Xbp1s protein in POMC neurons (Williams et al., 2014) to investigate the role of Cx43 in sympathetic innervation regulated WAT beiging. AGA has been used to uncouple gap junction channels in various cell culture models, via suggested mechanisms involving phosphorylation or changes in the aggregation of connexin subunits (Dhein, 2004; Le et al., 2014). Administration of AGA in the diet significantly reduces LY coupling in beige adipocytes (Suppl. Fig. 3A and 3B), suggesting the dose used in mice is effective. Two days of AGA exposure prompts a trend towards a reduction in Cx43, UCP1 and Cox7a1 gene expression in wildtype mice (Suppl. Fig. 3C).

Two weeks of Xbp1s overexpression in POMC neurons was previously shown to drastically increase WAT beiging for mice fed on a HFD (Williams et al., 2014). We treated the same mouse model with AGA (1g/kg in HFD diet containing 600 mg/kg doxycycline) while inducing Xbp1s expression (Fig. 5A). As expected, POMC Xbp1s expression reduces WAT weight by about 30%. In contrast, AGA treatment during the same time increases the fat pad weight by 26% (Fig. 5B). AGA treatment has no impact on the inguinal fat pad weight in control mice that lack expression of Xbp1s in POMC neurons (Fig. 5B). Trichrome staining and UCP-1 immunofluorescence staining further corroborate that AGA significantly reduces centrally-driven WAT beiging (Fig. 5C and 5D). A similar pattern was observed in the expression of WAT beiging signature genes, with all four genes measured displaying at least a 50% reduction after AGA treatment with a 90% reduction for UCP1 and Prdm16 expression (Fig. 5E). AGA failed to suppress beiging signature genes in control group, likely due to already suppressed expression levels of those genes after 2 weeks of HFD treatment.

WAT Specific Cx43 Overexpression Promotes Beiging at Room Temperature

Using a genetic model as well as a pharmacological inhibitor, we have implicated Cx43 channel activity in sympathetic neuronal signal-activated WAT beiging. Decreased Cx43 expression is observed in multiple tissues upon lipid overload, including in adipose tissues after a HFD challenge (Elmes et al., 2011; Keller et al., 2008; Noyan-Ashraf et al., 2013). Cx43 expression has an inverse correlation with glucose and insulin levels, and is implicated in aging and obesity in two mouse strains (Keller et al., 2008).

To complement the studies above, we decided to test whether Adeno-Associated Virus (AAV)-mediated WAT-specific Cx43 overexpression can promote WAT beiging at room temperature, a temperature that is considered to be below thermoneutrality for mice and causes a mild cold stress (Fig. 6A). 4 weeks after AAV injection directly into the fat pads, a 10-fold increase in Cx43 gene expression can be achieved (Fig. 6E); this is accompanied by about 7% reduction in fat pad weight compared to YFP-AAV virus injection in a control fat pad (Fig. 6B). Multiple beiging genes are upregulated in Cx43 AAV-injected fat pads (Fig. 6E). Histological analysis demonstrates an increase in WAT beiging in Cx43 AAV-injected fat pads (Fig. 6C and 6D). All of the mice in this cohort were single-housed at room temperature to reduce the variability in the individual degrees of WAT beiging.

A separate cohort of mice was injected with Cx43 and YFP AAV, but were housed at 30°C (Fig. 6H). Under thesese conditions, the Cx43 AAV mediated beiging effects were abolished (Fig. 6F–6J), while a similar level of Cx43 overexpression was achieved. This suggests that Cx43 amplifies sympathetic neuronal signals elicited by mild cold stress. Overexpression of Cx43 in the absence of sympathetic stimuli therefore does not promote WAT beiging.

In addition, we generated a mouse line that placed the mouse Cx43 gene (Gja1) under the TRE promoter. These mice (TRE-Cx43) were then crossed with adiponectin-rtTA mice and exposed to diet containing 10mg/kg doxycycline. Under these conditions, the mice displayed an increase of Cx43 at physiological levels, comparable to what can be seen after cold exposure in WAT (Fig. 6K and 6L). Those Cx43 transgenic mice also displayed a reduced fat pad weight, higher UCP1 expression and beiging of the WAT (Fig. 6N and 6O).

A Working Model of How Cx43 Facilitates the Propagation of WAT Beiging Signal

Cx43 is required for propagation of neuronal signals to induce beiging of WAT. We want to address the question whether adipocyte Cx43 expression is subject to neuronal regulation, and if so, how do sympathetic neuronal signals regulate Cx43 transcripts and channel activities? cAMP is a second messenger that is generated in cells receiving sympathetic neuronal input. cAMP activates the gap junction channel via phosphorylation and hemichannel assembly (Dhein, 2004; Nihei et al., 2010; TenBroek et al., 2001). Specifically, intracellular injection of cAMP enhances the cell-to-cell coupling in cardiac fibers (De Mello, 1984). Beyond direct activation of the gap junction channels, cAMP also increases Cx43 expression in the heart and in several cell lines (Dhein, 2004; Oyamada et al., 2013). In fact, this mechanism can be extended to adipocytes: a cell permeable cAMP analog 8-Bromo-cAMP treatment leads to a more than 2-fold increase in Cx43 expression (Fig. 7A)

and moderately increases UCP1 expression (Fig. 7A) in differentiated primary mouse adipocytes.

Based on our data and previously published literature, we propose a working model of cold-induced WAT beiging: cold-activated sympathetic nerves stimulate a subset of adipocytes via synapses, leading to an intracellular increase of cAMP, mitochondrial oxidative capacity and transdifferentiation to beige adipocytes. cAMP in turn upregulates Cx43 expression and assembly to allow enhanced diffusion to adjacent adipocytes that are not directly innervated by sympathetic nerves to elicit clusters of WAT beiging (Fig. 7B).

Discussion

Our studies describe the increase of Cx43 gap junction channel activity after neuronal stimulation as a vital step for proper beiging of WAT and the signal propagation from an adipocyte receiving a sympathetic signal to a cluster of adipocytes in close proximity. The expression of Cx43 is directly upregulated by cAMP in cultured adipocytes. Previous studies describe the activation and opening of the Cx43 channels by cAMP (Dhein, 2004). This represents a well-designed strategy for the central nervous system to actively control peripheral tissue metabolism in response to environmental cues. Interestingly, different connexin channels have distinct selectivity for negatively charged solutes involved in metabolic/biochemical coupling, and Cx43 channels show 7 to 10 times more permeability to cAMP than other channels such as those formed by Cx40 or Cx26 (Kanaporis et al., 2008). This may explain why Cx43 is the connexin of choice to be upregulated during WAT beiging.

Human brown-like fat depots can be induced in response to the cold, but this response is diminished in older and obese subjects (Ouellet et al., 2011). In rodents, increasing WAT beiging increases energy expenditure and opposes diet-induced obesity and glucose intolerance (Seale et al., 2011), whereas genetically blocking WAT beiging by deletion of critical factors such as Prdm16 promotes obesity and insulin resistance (Cohen et al., 2014; Seale et al., 2011). Notably, those brown-like fat depots in adult humans have molecular signatures more closely resembling rodent beige fat than classical brown fat (Lidell et al., 2013; Wu et al., 2012). Altogether, these studies suggest that promoting beige adipogenesis may be a viable strategy to improve metabolic phenotypes, certainly in rodents and potentially in humans.

Some studies suggest that WAT beiging can be a cell-autonomous process (Ye et al., 2013). Subcutaneous WAT normally responds to cold exposure with the release of free fatty acids and the induction of the beiging process, whereas dermal WAT (dWAT) reacts to the mild cold exposure with significant expansion of its thickness (up to 4-fold), (Kasza et al., 2014; Kruglikov and Scherer, 2016), suggesting a non-cell-automomous and likely neuronally controlled response of different fat depots in coordinating the response to the cold exposure. Additionally, fasting-induced activation of AgRP neurons can suppress cold-induced beiging, further highlighting the significance of neuronal control of WAT beiging (Ruan et al., 2014). As previously mentioned, WAT is not well innervated compared to BAT (Murano et al., 2009). Therefore, a strategy to maximize the interactions with clusters of adipocytes

for the effective propagation of neuronal signals in response to environmental stimuli is essential. In our studies, we identified Cx43 as a critical link in this process.

Another critical question is what the role of Cx43 is in lipolysis. One interesting observation is that fasting does not increase Cx43 expression in either WAT or BAT (Suppl. Fig. 4A, 4B). Fasting does not affect UCP1 levels either (Suppl. Fig. 4C, 4D), this is despite that fasting is a much stronger stimulus for WAT weight loss. We conclude that the role of Cx-43 in coupling adipocytes is cold-induced and beiging-specific.

In fact, regulation of Cx43 expression also plays an important role in white adipocyte development. *In vitro* adipogenesis can be classified into 3 stages: mitotic clonal expansion, differentiation and lipid droplet accumulation. Gap junctions, especially Cx43 are required for the mitotic clonal expansion (Yanagiya et al., 2007). However, elimination of gap junctional activity is required for late stage adipocyte maturation, especially for lipid droplet accumulation (Azarnia and Russell, 1985; Yeganeh et al., 2012). The addition of dibutyryl cyclic AMP to already differentiated adipocytes resulted in a loss of lipid droplets and simultaneously increased junctional permeability, although no specific connexin was identified in this study (Azarnia and Russell, 1985). The changes in junctional permeability during the SVF differentiation process coincide with the changes in Cx43 expression levels (Fig. 7C), suggesting that Cx43 is the major connexin protein in this physiological process. This inverse correlation between Cx43 levels and lipid droplet accumulation suggests a critical role for eliminating Cx43 and gap junction activity in lipid accumulation during the final stages of adipocyte differentiation.

Additionally, there are numerous positive correlations of increased adipogenesis with inhibition or loss of Cx43 channel activity in many different cell types beyond adipocytes. For example, inhibition of Cx43 by AGA induces phenotypic changes of skeletal muscle cells to enter adipogenesis (Yamanouchi et al., 2007). Inhibition of gap junctional communication induces the trans-differentiation of osteoblasts to an adipocytic phenotype *in vitro* (Schiller et al., 2001). Similarly, a genetic mouse model with a Cx43 loss of function mutation leads to extensive adipogenesis in bone marrow (Zappitelli et al., 2015), further cementing the strong correlation between the inhibition of gap junctional activity and the degree of adipogenesis in multipotent cells that have the capacity to undergo adipogenesis. In contrast, the TRPV1 agonist capsaicin increases Cx43 in mesenteric fat, and improves metabolic function during diet-induced-obesity (Chen et al., 2015), even though a direct role in the metabolic improvements is hard to prove in this context. All of these phenotypic observations firmly highlight the inverse correlation of Cx43 levels, adipogenesis and lipid accumulation. It remains unknown whether all these different cell types actively suppress adipogenesis through a neuronal mechanism, and the degradation of Cx43 isolates individual cells from that inhibitory neuronal activity. Alternatively, Cx43 may inhibit adipogenesis and lipid accumulation independent of it gap junctional activities, which is beyond the scope of this paper.

A comprehensive gene expression analysis of *ob/ob* vs control mice at two different ages revealed an inverse correlation of Cx43 levels with serum glucose and insulin, indicating a role of Cx43 in obesity for both the B6 and the BTBR mouse strains (Fig. 7D) (Keller et al.,

2008). The difference in Cx43 immunofluorescence signal between human deep neck fat (beige/brown adipose) and white adipose tissue (Fig. 7E) and the differentiated gene expression levels between the two fat depots (Fig. 7F) both confirm the positive correlation of Cx43 with tissue oxidative capacity in human subjects as well. Intuitively, a pharmacologic increase of Cx43 expression or activation of Cx43 channels may be an effective approach to combat lipid accumulation in obesity and other metabolic diseases.

In summary, we used both genetic models and pharmacologic methods to achieve gain-of-function and loss-of-function of Cx43 gap junction activity during WAT beiging. We demonstrate that Cx43 is necessary and sufficient in propagating a sympathetic neuronal signal to mediate WAT beiging. We identified Cx43 as the major connexin isoform in the regulation of this junctional activity in response to sympathetic neuronal signals. These observations fill a gap in our understanding of how neuronal signals regulate peripheral responses to environmental cues in a timely manner. It also suggests that approaches aimed at pharmacological increases and activation of Cx43 may hold promise to manipulate WAT beiging and potentially improve whole body glucose homeostasis.

EXPERIMENTAL PROCEDURES

Mice

Connexin 43 (Gja1) floxed mice (#008039) and TRE-Cre mice (#006234) on the C57BL/6 background were purchased from the Jackson Laboratory. UCP-1 rtTA (Sun et al., 2014) mice and TRE-Cx43 mice were generated and characterized in our laboratory. They were on a pure C57BL/6 background. All animals were kept on a 12 hr light-dark cycle in a temperature-controlled environment (room temperature: 22°C, cold: 6°C or thermoneutrality: 30°C). Mice were free to access water and either fed on a standard chow diet or 60% high fat diet with or without indicated amount (10 mg/kg or 600 mg/kg) doxycycline (BioServ). AGA (1g/kg, Sigma) was blended into the diet for the indicated times. All animal procedures have been approved by the Institutional Animal Care and Use Committee of UT Southwestern Medical Center at Dallas.

Human Subjects

Human omental adipose tissue samples were collected from metabolically healthy obese patients who underwent bariatric surgery at the University of Texas Southwestern Medical Center (UT Southwestern). Details on collection of the deep neck adipose tissue samples were described previously (Cypess et al., 2013). The tissue collection followed the institutional guidelines and was approved by the Institutional Review Boards of UT Southwestern. All subjects gave written informed consent before taking part in the study.

Lucifer Yellow Dye Coupling

The experimental procedure was adapted from a previous publication (Burke et al., 2014). Briefly, experiments were performed using an upright microscope (Nikon Eclipse FN1) equipped with a fixed stage and a QuantEM:512SC electron-multiplying charge-coupled device camera, connected to a computer running NIS-Elements AR 3.2 proprietary imaging software. Freshly collected mouse WATs were dissected in patch buffer (110 mM NaCl, 4.7

mM KCl, 14.4 mM NaHCO3, 1.2 mM MgSO4, 1.2 mM NaH2PO4, 2.5 mM CaCl2 and11.5 mM glucose, at pH 7.3 and bubbled with 95%O_2/5% CO_2.). Individual adipocytes were visualized and injected with the fluorescent dye Lucifer Yellow (Sigma) 2.5% in 0.5 M LiCl from micropipettes. The dye-injected cells and their neighbor cells were imaged with the digital camera 10 minutes after the dye injection. Multiple injections from tissues collected from at least 3 different mice were used for quantification.

Metabolic Measurements

Glucose tolerance tests (1.25 g/kg glucose was used for lean mice, 0.75 g/kg glucose was used for obese mice) and blood glucose were performed as described previously (Wang et al., 2015). Serum parameters (Albumin, Aspartate transaminase, Alanine transaminase, Bilirubin, Cholesterol, Triglyceride, and Direct high density lipoprotein) were measured by a VITROS analyzer (Ortho Clinical Diagnostics) at UT Southwestern metabolic phenotyping core.

Sympathetic Denervation

Mice received 10 micro injections of vehicle or 6-hydroxydopamine [6-OHDA (Sigma)] 1 μl per injection, 9 mg/ml in 0.15 M NaCl containing 1% (w/v) ascorbic acid] per each inguinal fat pad after isoflurane anesthesia as described previously (Chao et al., 2011).

Other Experimental Procedures

Immunofluorescence, rAAV Vector Construction and Packaging, Gene Expression Analysis, SVF Culture and Adipocyte Differentiation, Body Temperature Measurements and Liver Lipid Assays are described in Supplemental Information.

Statistical Analysis

Results are shown as mean ± SEM. Unless otherwise indicated, the comparisons were carried out using unpaired Student’s t test or one-way ANOVA followed by post hoc comparisons using Bonferroni post-hoc test. p values <0.05 were considered statistically significant.

Supplementary Material

Refer to Web version on PubMed Central for supplementary material.

Acknowledgments

This study was supported by NIH Grants R01-DK55758, R01-DK099110 and P01-DK088761 as well as a grant from the Cancer Prevention and Research Institute of Texas (CPRIT RP140412) to P.E.S., Lilly Innovation Fellowship Award (LIFA) to Y.Z., China Scholarship Council 201406280111 to T.Y., AHA 14SDG20370016 to T.L., NIH Grant R03-DK101865 to O.G., NIH Grant R01-NS092466 to D.C.S., NIH Grant R21-AI124000 to H.B.T., NIH Grants R01-CA163640, R01-CA166590, and R21-CA178227 to L.C., NIH R01-DK077097 and R01-DK102898 to Y.-H.T., NIH Grants R37-DK053301, R01-DK088423, R01-DK100659 and P01-DK088761 to J.K.E., NIH Grant R01-DK100699 to K.W.W., NIH Grant R01-DK104789 to R.K.G., and NIH R00-DK094973 to W.L.H.

References

Azarnia R, Russell TR. Cyclic AMP effects on cell-to-cell junctional membrane permeability during adipocyte differentiation of 3T3-L1 fibroblasts. J Cell Biol. 1985; 100:265–269. [PubMed: 2981232]

Bartelt A, Heeren J. Adipose tissue browning and metabolic health. Nat Rev Endocrinol. 2014; 10:24–36. [PubMed: 24146030]

Burke S, Nagajyothi F, Thi MM, Hanani M, Scherer PE, Tanowitz HB, Spray DC. Adipocytes in both brown and white adipose tissue of adult mice are functionally connected via gap junctions: implications for Chagas disease. Microbes Infect. 2014; 16:893–901. [PubMed: 25150689]

Cannon B, Nedergaard J. Brown adipose tissue: function and physiological significance. Physiol Rev. 2004; 84:277–359. [PubMed: 14715917]

Chao PT, Yang L, Aja S, Moran TH, Bi S. Knockdown of NPY expression in the dorsomedial hypothalamus promotes development of brown adipocytes and prevents diet-induced obesity. Cell Metab. 2011; 13:573–583. [PubMed: 21531339]

Chen J, Li L, Li Y, Liang X, Sun Q, Yu H, Zhong J, Ni Y, Zhao Z, Gao P, et al. Activation of TRPV1 channel by dietary capsaicin improves visceral fat remodeling through connexin43-mediated Ca2+ Influx. Cardiovasc Diabetol. 2015; 14:22. [PubMed: 25849380]

Cohen P, Levy JD, Zhang Y, Frontini A, Kolodin DP, Svensson KJ, Lo JC, Zeng X, Ye L, Khandekar MJ, et al. Ablation of PRDM16 and beige adipose causes metabolic dysfunction and a subcutaneous to visceral fat switch. Cell. 2014; 156:304–316. [PubMed: 24439384]

Cypess AM, Lehman S, Williams G, Tal I, Rodman D, Goldfine AB, Kuo FC, Palmer EL, Tseng YH, Doria A, et al. Identification and importance of brown adipose tissue in adult humans. N Engl J Med. 2009; 360:1509–1517. [PubMed: 19357406]

Cypess AM, White AP, Vernochet C, Schulz TJ, Xue R, Sass CA, Huang TL, Roberts-Toler C, Weiner LS, Sze C, et al. Anatomical localization, gene expression profiling and functional characterization of adult human neck brown fat. Nat Med. 2013; 19:635–639. [PubMed: 23603815]

Dalziel K. The nervous system and adipose tissue. Clin Dermatol. 1989; 7:62–77. [PubMed: 2691052]

De Mello WC. Effect of intracellular injection of cAMP on the electrical coupling of mammalian cardiac cells. Biochem Biophys Res Commun. 1984; 119:1001–1007. [PubMed: 6324775]

Dhein S. Pharmacology of gap junctions in the cardiovascular system. Cardiovasc Res. 2004; 62:287–298. [PubMed: 15094349]

Dodd GT, Decherf S, Loh K, Simonds SE, Wiede F, Balland E, Merry TL, Munzberg H, Zhang ZY, Kahn BB, et al. Leptin and insulin act on POMC neurons to promote the browning of white fat. Cell. 2015; 160:88–104. [PubMed: 25594176]

Elmes MJ, Tan DS, Cheng Z, Wathes DC, McMullen S. The effects of a high-fat, high-cholesterol diet on markers of uterine contractility during parturition in the rat. Reproduction. 2011; 141:283–290. [PubMed: 21078880]

Enerback S, Jacobsson A, Simpson EM, Guerra C, Yamashita H, Harper ME, Kozak LP. Mice lacking mitochondrial uncoupling protein are cold-sensitive but not obese. Nature. 1997; 387:90–94. [PubMed: 9139827]

Kanaporis G, Mese G, Valiuniene L, White TW, Brink PR, Valiunas V. Gap junction channels exhibit connexin-specific permeability to cyclic nucleotides. J Gen Physiol. 2008; 131:293–305. [PubMed: 18378798]

Kasza I, Suh Y, Wollny D, Clark RJ, Roopra A, Colman RJ, MacDougald OA, Shedd TA, Nelson DW, Yen MI, et al. Syndecan-1 is required to maintain intradermal fat and prevent cold stress. PLoS Genet. 2014; 10:e1004514. [PubMed: 25101993]

Kazak L, Chouchani ET, Jedrychowski MP, Erickson BK, Shinoda K, Cohen P, Vetrivelan R, Lu GZ, Laznik-Bogoslavski D, Hasenfuss SC, et al. A Creatine-Driven Substrate Cycle Enhances Energy Expenditure and Thermogenesis in Beige Fat. Cell. 2015; 163:643–655. [PubMed: 26496606]

Keller MP, Choi Y, Wang P, Davis DB, Rabaglia ME, Oler AT, Stapleton DS, Argmann C, Schueler KL, Edwards S, et al. A gene expression network model of type 2 diabetes links cell cycle regulation in islets with diabetes susceptibility. Genome Res. 2008; 18:706–716. [PubMed: 18347327]

Kruglikov IL, Scherer PE. Dermal Adipocytes: From Irrelevance to Metabolic Targets? Trends Endocrinol Metab. 2016; 27:1–10. [PubMed: 26643658]

Le HT, Sin WC, Lozinsky S, Bechberger J, Vega JL, Guo XQ, Saez JC, Naus CC. Gap junction intercellular communication mediated by connexin43 in astrocytes is essential for their resistance to oxidative stress. J Biol Chem. 2014; 289:1345–1354. [PubMed: 24302722]

Lidell ME, Betz MJ, Dahlqvist Leinhard O, Heglind M, Elander L, Slawik M, Mussack T, Nilsson D, Romu T, Nuutila P, et al. Evidence for two types of brown adipose tissue in humans. Nat Med. 2013; 19:631–634. [PubMed: 23603813]

Murano I, Barbatelli G, Giordano A, Cinti S. Noradrenergic parenchymal nerve fiber branching after cold acclimatisation correlates with brown adipocyte density in mouse adipose organ. J Anat. 2009; 214:171–178. [PubMed: 19018882]

Nihei OK, Fonseca PC, Rubim NM, Bonavita AG, Lyra JS, Neves-dos-Santos S, de Carvalho AC, Spray DC, Savino W, Alves LA. Modulatory effects of cAMP and PKC activation on gap junctional intercellular communication among thymic epithelial cells. BMC Cell Biol. 2010; 11:3. [PubMed: 20078861]

Noyan-Ashraf MH, Shikatani EA, Schuiki I, Mukovozov I, Wu J, Li RK, Volchuk A, Robinson LA, Billia F, Drucker DJ, et al. A glucagon-like peptide-1 analog reverses the molecular pathology and cardiac dysfunction of a mouse model of obesity. Circulation. 2013; 127:74–85. [PubMed: 23186644]

Ouellet V, Routhier-Labadie A, Bellemare W, Lakhal-Chaieb L, Turcotte E, Carpentier AC, Richard D. Outdoor temperature, age, sex, body mass index, and diabetic status determine the prevalence, mass, and glucose-uptake activity of 18F-FDG-detected BAT in humans. J Clin Endocrinol Metab. 2011; 96:192–199. [PubMed: 20943785]

Oyamada M, Takebe K, Oyamada Y. Regulation of connexin expression by transcription factors and epigenetic mechanisms. Biochim Biophys Acta. 2013; 1828:118–133. [PubMed: 22244842]

Petrovic N, Walden TB, Shabalina IG, Timmons JA, Cannon B, Nedergaard J. Chronic peroxisome proliferator-activated receptor gamma (PPARgamma) activation of epididymally derived white adipocyte cultures reveals a population of thermogenically competent, UCP1-containing adipocytes molecularly distinct from classic brown adipocytes. J Biol Chem. 2010; 285:7153–7164. [PubMed: 20028987]

Rosen ED, Spiegelman BM. Adipocytes as regulators of energy balance and glucose homeostasis. Nature. 2006; 444:847–853. [PubMed: 17167472]

Ruan HB, Dietrich MO, Liu ZW, Zimmer MR, Li MD, Singh JP, Zhang K, Yin R, Wu J, Horvath TL, et al. O-GlcNAc transferase enables AgRP neurons to suppress browning of white fat. Cell. 2014; 159:306–317. [PubMed: 25303527]

Schiller PC, D'Ippolito G, Brambilla R, Roos BA, Howard GA. Inhibition of gap-junctional communication induces the trans-differentiation of osteoblasts to an adipocytic phenotype in vitro. J Biol Chem. 2001; 276:14133–14138. [PubMed: 11278824]

Schneider-Picard G, Carpentier JL, Orci L. Quantitative evaluation of gap junctions during development of the brown adipose tissue. J Lipid Res. 1980; 21:600–607. [PubMed: 7400690]

Seale P, Conroe HM, Estall J, Kajimura S, Frontini A, Ishibashi J, Cohen P, Cinti S, Spiegelman BM. Prdm16 determines the thermogenic program of subcutaneous white adipose tissue in mice. J Clin Invest. 2011; 121:96–105. [PubMed: 21123942]

Spiegelman BM, Flier JS. Obesity and the regulation of energy balance. Cell. 2001; 104:531–543. [PubMed: 11239410]

Stout RF Jr, Snapp EL, Spray DC. Connexin Type and Fluorescent Protein Fusion Tag Determine Structural Stability of Gap Junction Plaques. J Biol Chem. 2015; 290:23497–23514. [PubMed: 26265468]

Sun K, Kusminski CM, Luby-Phelps K, Spurgin SB, An YA, Wang QA, Holland WL, Scherer PE. Brown adipose tissue derived VEGF-A modulates cold tolerance and energy expenditure. Mol Metab. 2014; 3:474–483. [PubMed: 24944907]

TenBroek EM, Lampe PD, Solan JL, Reynhout JK, Johnson RG. Ser364 of connexin43 and the upregulation of gap junction assembly by cAMP. J Cell Biol. 2001; 155:1307–1318. [PubMed: 11756479]

van Marken Lichtenbelt WD, Vanhommerig JW, Smulders NM, Drossaerts JM, Kemerink GJ, Bouvy ND, Schrauwen P, Teule GJ. Cold-activated brown adipose tissue in healthy men. N Engl J Med. 2009; 360:1500–1508. [PubMed: 19357405]

Virtanen KA, Lidell ME, Orava J, Heglind M, Westergren R, Niemi T, Taittonen M, Laine J, Savisto NJ, Enerback S, et al. Functional brown adipose tissue in healthy adults. N Engl J Med. 2009; 360:1518–1525. [PubMed: 19357407]

Wang QA, Tao C, Gupta RK, Scherer PE. Tracking adipogenesis during white adipose tissue development, expansion and regeneration. Nat Med. 2013; 19:1338–1344. [PubMed: 23995282]

Wang QA, Tao C, Jiang L, Shao M, Ye R, Zhu Y, Gordillo R, Ali A, Lian Y, Holland WL, et al. Distinct regulatory mechanisms governing embryonic versus adult adipocyte maturation. Nat Cell Biol. 2015; 17:1099–1111. [PubMed: 26280538]

Weber PA, Chang HC, Spaeth KE, Nitsche JM, Nicholson BJ. The permeability of gap junction channels to probes of different size is dependent on connexin composition and permeant-pore affinities. Biophys J. 2004; 87:958–973. [PubMed: 15298902]

Williams KW, Liu T, Kong X, Fukuda M, Deng Y, Berglund ED, Deng Z, Gao Y, Sohn JW, Jia L, et al. Xbp1s in Pomc neurons connects ER stress with energy balance and glucose homeostasis. Cell Metab. 2014; 20:471–482. [PubMed: 25017942]

Wu J, Bostrom P, Sparks LM, Ye L, Choi JH, Giang AH, Khandekar M, Virtanen KA, Nuutila P, Schaart G, et al. Beige adipocytes are a distinct type of thermogenic fat cell in mouse and human. Cell. 2012; 150:366–376. [PubMed: 22796012]

Wu J, Cohen P, Spiegelman BM. Adaptive thermogenesis in adipocytes: is beige the new brown? Genes Dev. 2013; 27:234–250. [PubMed: 23388824]

Yamanouchi K, Yada E, Ishiguro N, Nishihara M. 18alpha-glycyrrhetinic acid induces phenotypic changes of skeletal muscle cells to enter adipogenesis. Cell Physiol Biochem. 2007; 20:781–790. [PubMed: 17982260]

Yanagiya T, Tanabe A, Hotta K. Gap-junctional communication is required for mitotic clonal expansion during adipogenesis. Obesity (Silver Spring). 2007; 15:572–582. [PubMed: 17372306]

Ye L, Wu J, Cohen P, Kazak L, Khandekar MJ, Jedrychowski MP, Zeng X, Gygi SP, Spiegelman BM. Fat cells directly sense temperature to activate thermogenesis. Proc Natl Acad Sci U S A. 2013; 110:12480–12485. [PubMed: 23818608]

Yeganeh A, Stelmack GL, Fandrich RR, Halayko AJ, Kardami E, Zahradka P. Connexin 43 phosphorylation and degradation are required for adipogenesis. Biochim Biophys Acta. 2012; 1823:1731–1744. [PubMed: 22705883]

Zappitelli T, Chen F, Aubin JE. Up-regulation of BMP2/4 signaling increases both osteoblast-specific marker expression and bone marrow adipogenesis in Gja1Jrt/+ stromal cell cultures. Mol Biol Cell. 2015; 26:832–842. [PubMed: 25568340]

Zeng W, Pirzgalska RM, Pereira MM, Kubasova N, Barateiro A, Seixas E, Lu YH, Kozlova A, Voss H, Martins GG, et al. Sympathetic Neuro-adipose Connections Mediate Leptin-Driven Lipolysis. Cell. 2015; 163:84–94. [PubMed: 26406372]

Highlights

- Cx43 expression and beige adipocyte gap junctions are increased during WAT beiging.
- Genetic disruption or pharmacological inhibition of Cx43 blunts WAT beiging.
- Overexpression Cx43 promotes WAT beiging in the presence of a mild cold stimulus.
- Human beige/brown fat has higher Cx43 expression compared to white adipose tissue.

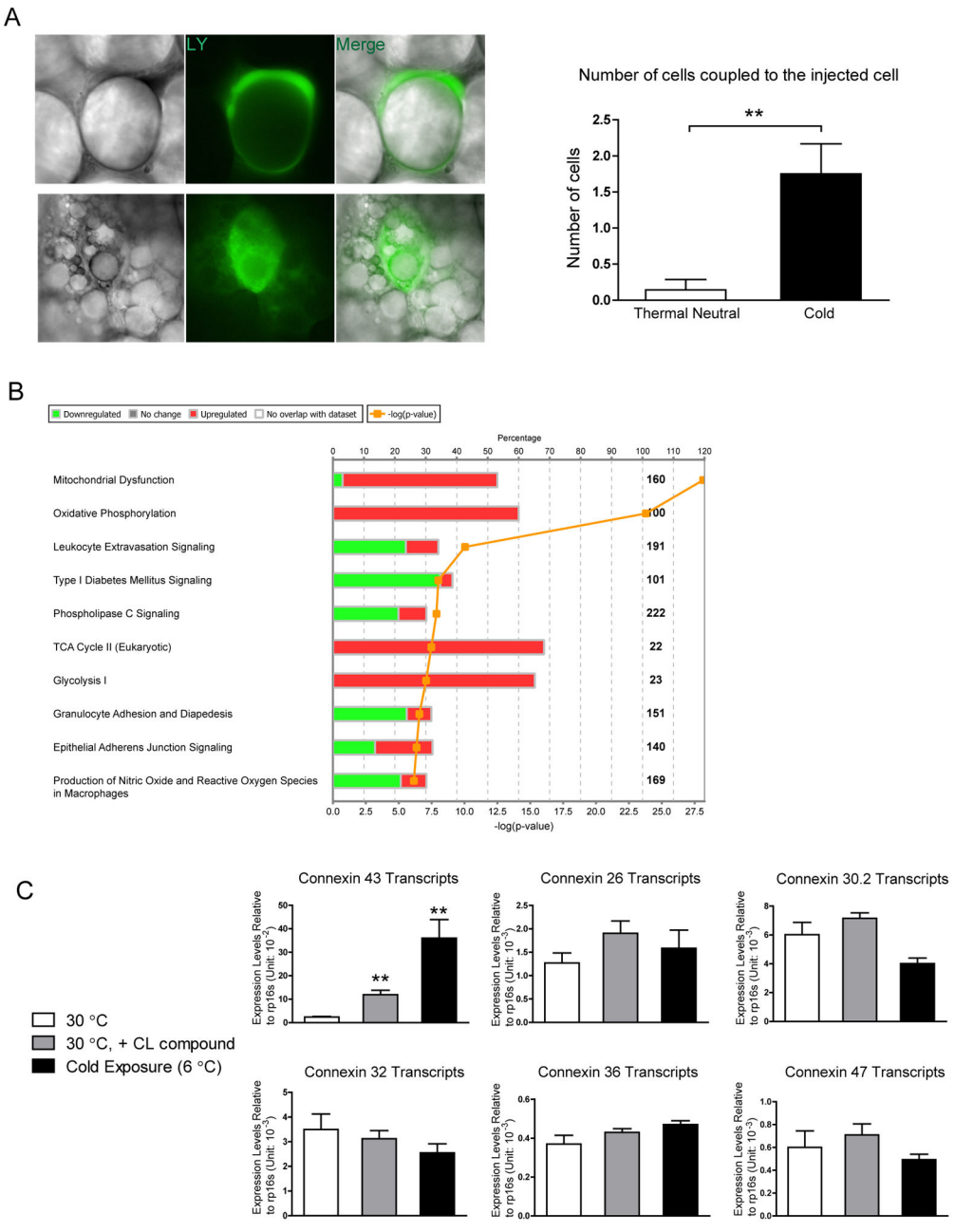

Figure 1. Increased Gap Junction Activity and Cx43 Expression during WAT Beiging

A. Lucifer yellow coupling experiment, upper panel: adipocytes from mice kept at thermoneutrality; lower panel: beige adipocytes from mice kept at 6°C for 3 days. Quantification of the average number of cells coupled to the injected cell is shown on the right. n = 7 for adipocytes from mice housed at thermoneutrality, n = 10 for beige adipocytes. **B.** Pathway analysis of genes changed in the microarray study (cold treatment/ thermoneutrality, mouse subcutaneous fat pad). **C**. Gene expression of various connexins in adipose tissue from mice at thermoneutrality, thermoneutrality and receiving CL316,243

treatment, or mice housed in the cold (n = 4–5). Results are shown as mean ± SEM, **p < 0.01.

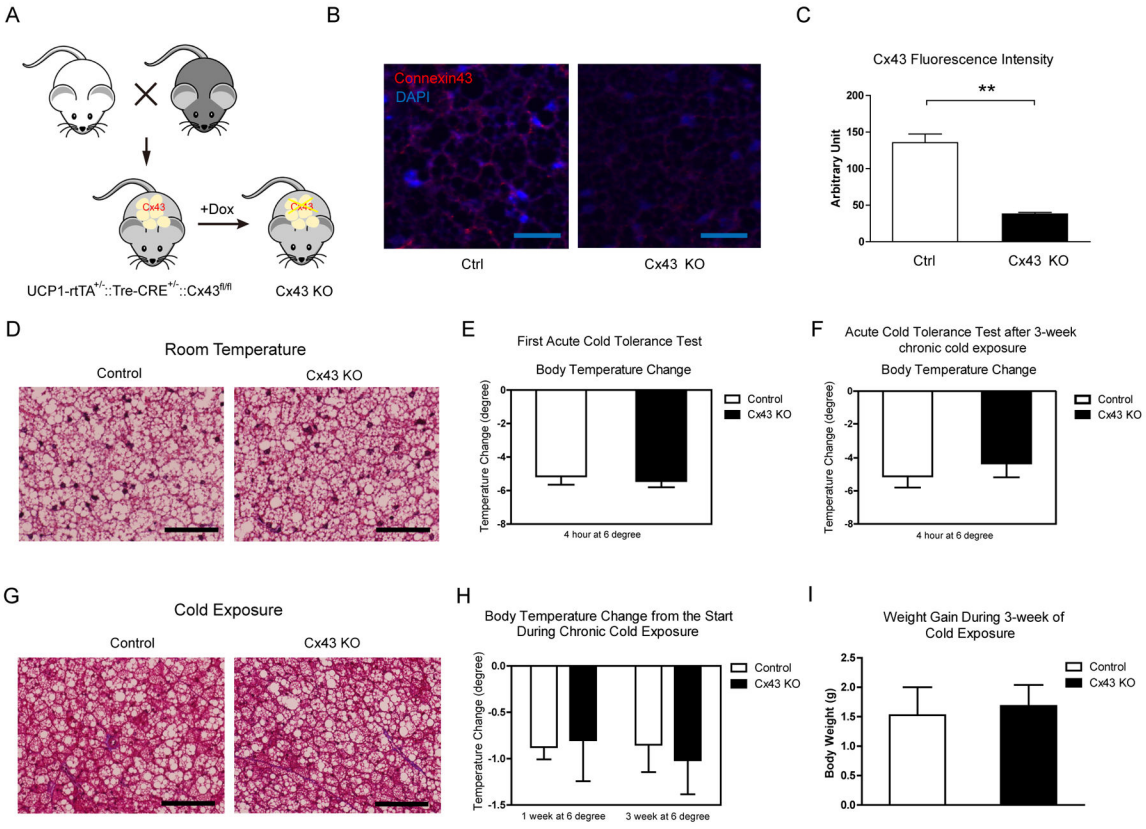

Figure 2. UCP-1 Promoter Driven Cx43 Deletion Does Not Affect BAT Physiology and Thermal Adaptation to the Cold

A. Schematic of the mouse model. **B.** Representative confocal images of anti-Cx43 immunofluorescence staining. Scale bar = 25 μm. **C.** Quantification of Cx43 fluorescent signals (n = 8). **D.** Trichrome staining of BAT from mice housed at room temperature. Scale bar = 50 μm. **E.** Acute cold tolerance test (n = 5–6). **F.** Repeat acute cold tolerance test of the mice previously exposed to the cold for 3 weeks (n = 5–6). **G.** Trichrome staining of BAT from mice exposed to the cold for 3 weeks. Scale bar = 50 μm. **H.** Body temperature change during the chronic cold exposure (n = 5–6). **I.** Body weight gain during 3-week cold exposure (n = 5–6). Results are shown as mean ± SEM, *p < 0.05.

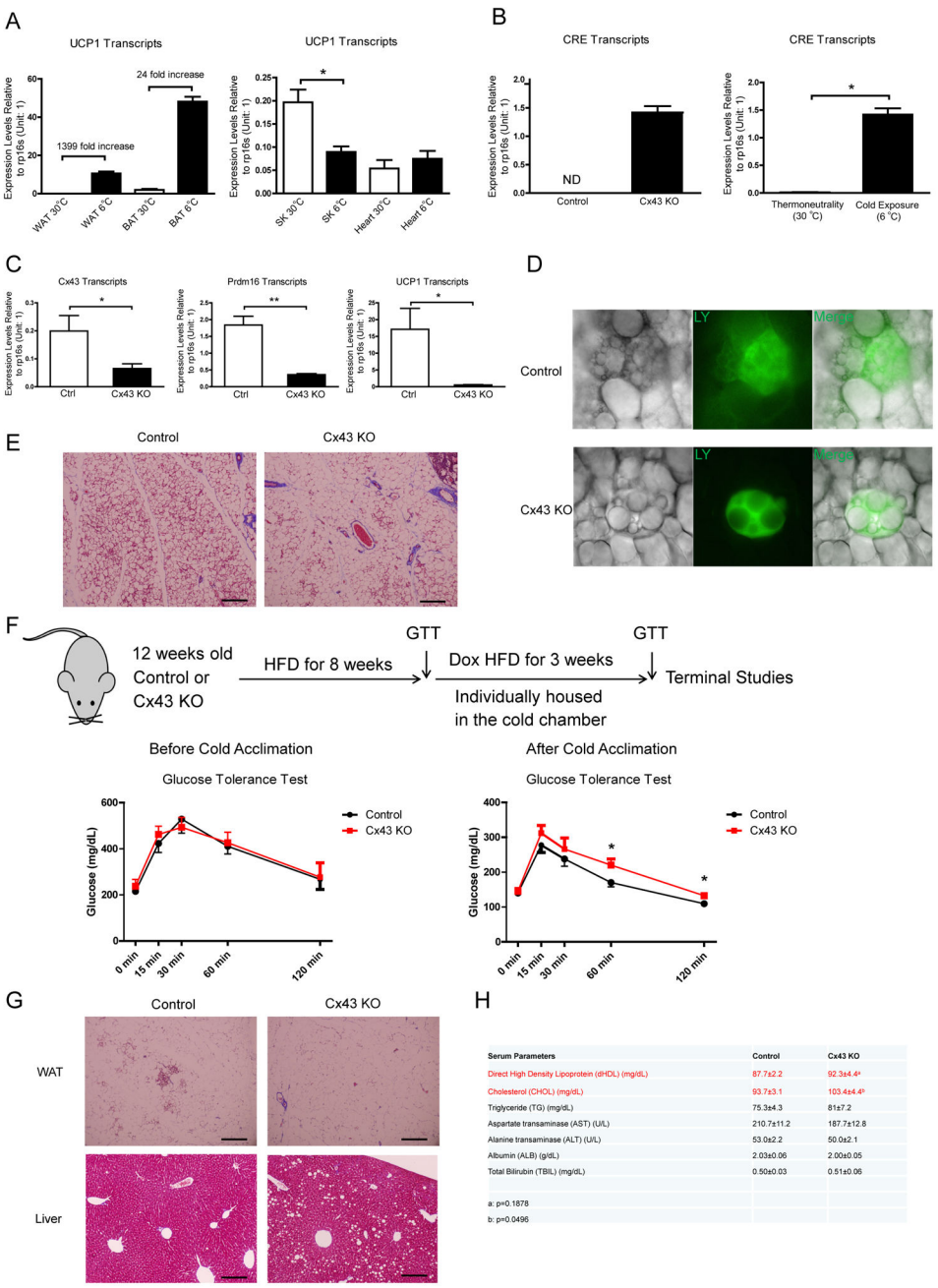

Serum Parameters	Control	Cx43 KO
Direct High Density Lipoprotein (dHDL) (mg/dL)	87.7±2.2	92.3±4.4[a]
Cholesterol (CHOL) (mg/dL)	93.7±3.1	103.4±4.4[b]
Triglyceride (TG) (mg/dL)	75.3±4.3	81±7.2
Aspartate transaminase (AST) (U/L)	210.7±11.2	187.7±12.8
Alanine transaminase (ALT) (U/L)	53.0±2.2	50.0±2.1
Albumin (ALB) (g/dL)	2.03±0.06	2.00±0.05
Total Bilirubin (TBIL) (mg/dL)	0.50±0.03	0.51±0.06

a: p=0.1878

b: p=0.0496

Figure 3. UCP1 Promoter-Driven Cx43 Deletion Blunts Cold Induced Metabolic Improvements

A. UCP1 transcripts in various metabolic tissues after 48-hour cold exposure (n = 4). WAT: white adipose tissue; BAT: brown adipose tissue, SK: skeletal muscle. **B.** CRE expression in WAT after 48-hour cold exposure (n = 2–3). **C.** Cx43, Prdm16, UCP1 expression levels in WAT after 48-hour cold exposure (n = 4). **D.** Lucifer Yellow coupling experiments in control and Cx43-KO beige adipocytes. **E.** Trichrome staining of control and Cx43-KO WAT after a 3-day cold exposure. **F.** Schematic of mouse treatment regimen, GTTs before (n = 4–7) and after (n = 6–7) cold exposure. **G.** Trichrome staining of WAT and Liver from mice referred

in Panel F. **H.** Serum lipid profiles and liver enzymes from the mice referred in Panel F (n = 6–7). Scale bar = 100 μm. Results are shown as mean ± SEM, *p<0.05, **p < 0.01.

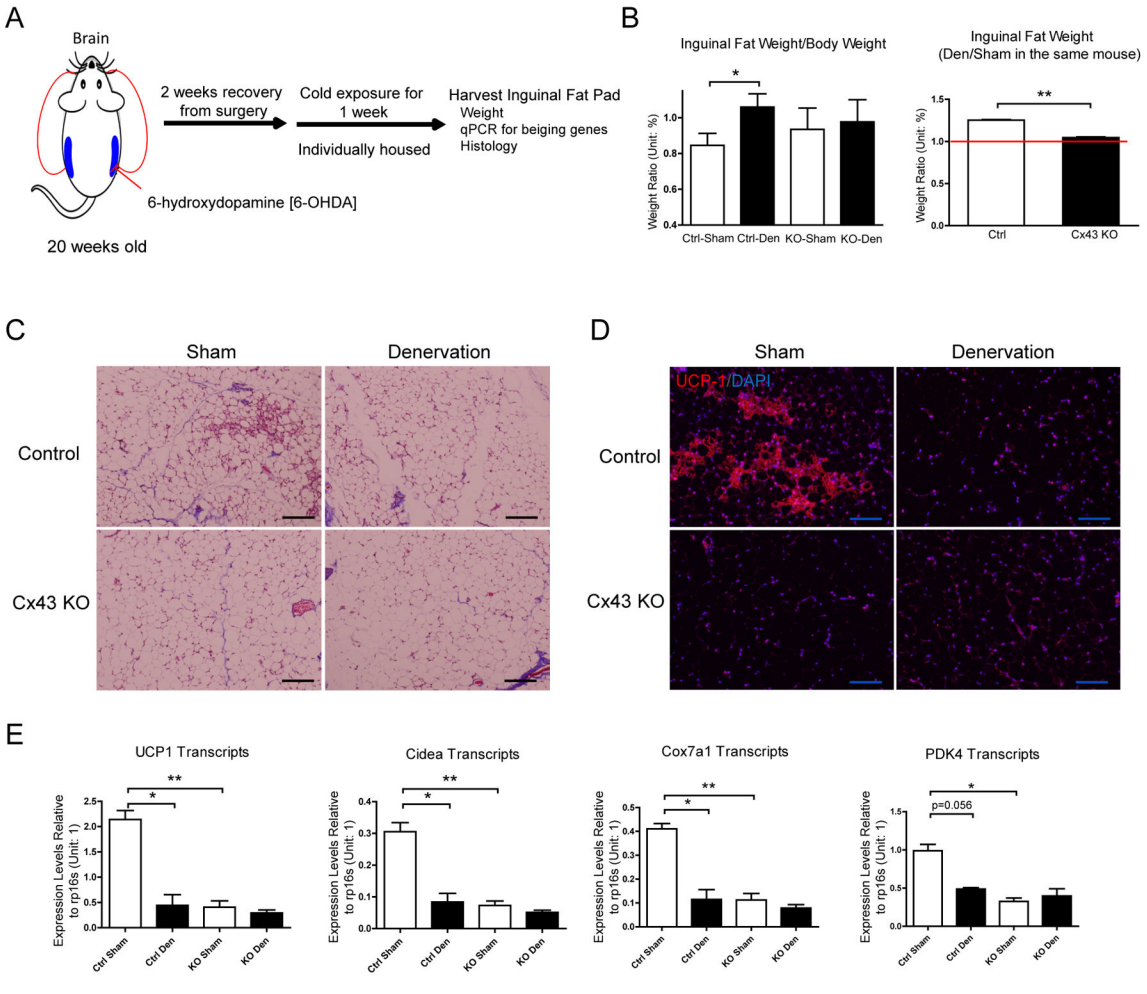

Figure 4. UCP1-driven Cx43 Deletion Impairs WAT Beiging to a Similar Level as upon WAT Denervation

A. Schematic of denervation experiment procedure. **B.** Inguinal fat pad weight after denervation and cold exposure (n = 4–5). **C.** Trichrome staining. **D.** UCP1 immunofluorescent staining. **E.** Expression of beiging signature genes (n = 6–11). Scale bar = 100 μm. Results are shown as mean ± SEM, *p<0.05, **p < 0.01.

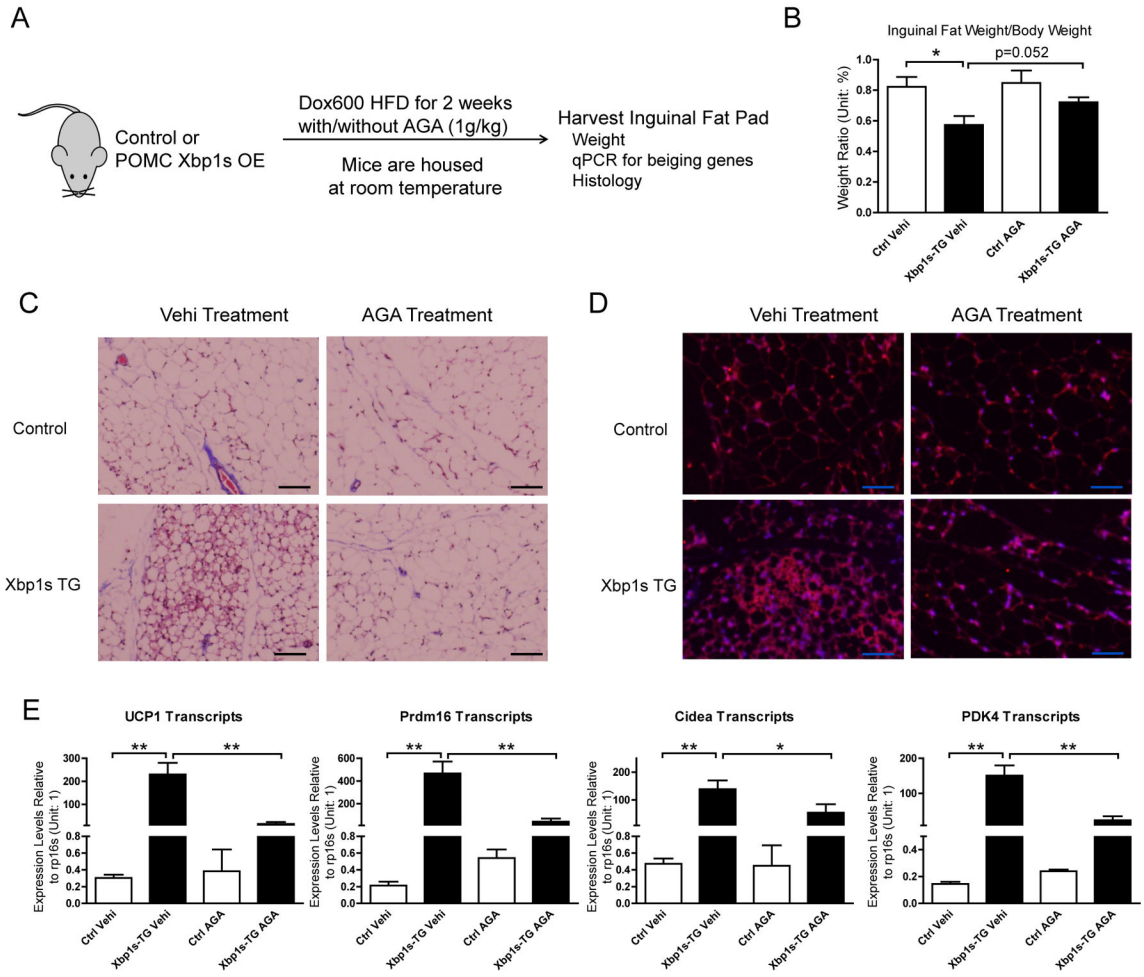

Figure 5. Blocking of Cx43 Channels by 18α-Glycyrrhetinic acid (AGA) Inhibits Sympathetic Activation-Induced WAT Beiging

A. Schematic of mouse treatment: Control or tet-inducible POMC neuron specific Xbp1s overexpression (OE) mice were exposed to Dox600 HFD for transgene expression while at the same time treated with or without AGA compound at 1g/kg dose in diet. Dox600 HFD containing no AGA compound is considered vehicle (Vehi). Mice were housed at room temperature and sacrificed at the end of 2 weeks, inguinal fat tissues from experimental mice were harvested for tissue weight measurements, mRNA extraction and histological analysis. **B.** Inguinal fat pad weight from mice treated with AGA (n = 5–7). **C.** Trichrome staining. **D.** UCP1 immunofluorescent staining. **E.** Expression of beiging signature genes (n = 8). Scale bar = 50 μm. Results are shown as mean ± SEM, *p<0.05, **p < 0.01.

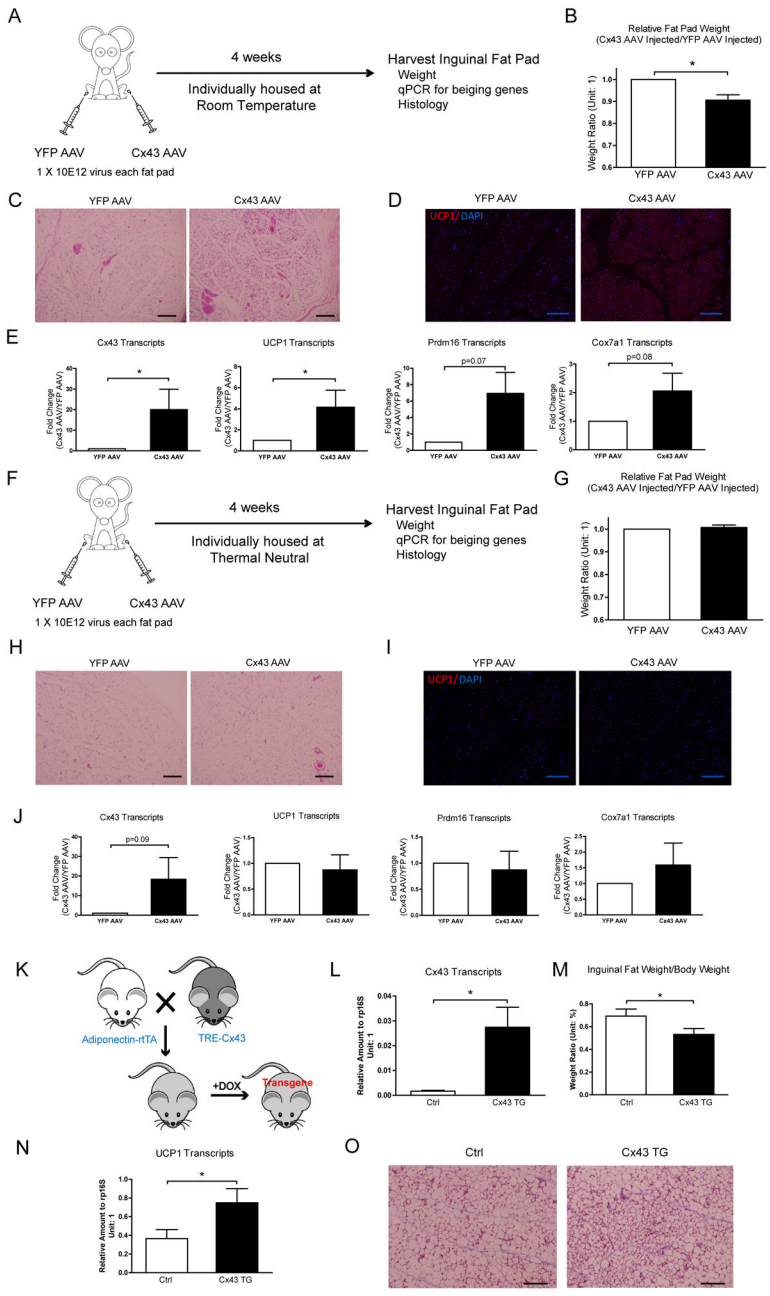

Figure 6. WAT Specific Cx43 Overexpression Promotes Beiging at Room Temperature

A. Schematic of mouse treatments and experimental procedures for the cohort housed at room temperature. **B.** Cx43 AAV infected inguinal fat pad weights, normalized to YFP AAV injected fat pad weights in the same mouse (n = 3). **C.** H&E staining. **D.** UCP1 staining. **E.** Expression of Cx43 and WAT beiging signature genes (n = 3). Data are presented as fold changes to mRNA abundance in YFP AAV control samples. **F.** Schematic of mouse treatments and experimental procedure for the cohort kept at thermoneutrality. **G.** Cx43 AAV infected inguinal fat pad weights, normalized to YFP AAV injected fat pad weights in the same mouse (n = 3). **H.** H&E staining. **I.** UCP1 staining. **J.** Expression of Cx43 and

WAT beiging signature genes (n = 3). Data are presented as fold changes to mRNA abundance in YFP AAV control samples. **K.** Schematic of mouse cross and treatments. **L.** Expression of Cx43 in Control (Ctrl) and Cx43 transgenic (Cx43 TG) after doxycycline induction for 3 days (n = 4). **M.** Inguinal fat pad weight normalized to body weight (n = 4). **N.** Expression of UCP1 in Ctrl and Cx43 TG after doxycycline induction for 3 days (n = 4). **O.** Trichrome staining. Scale bar = 100 μm. Results are shown as mean ± SEM, *p<0.05.

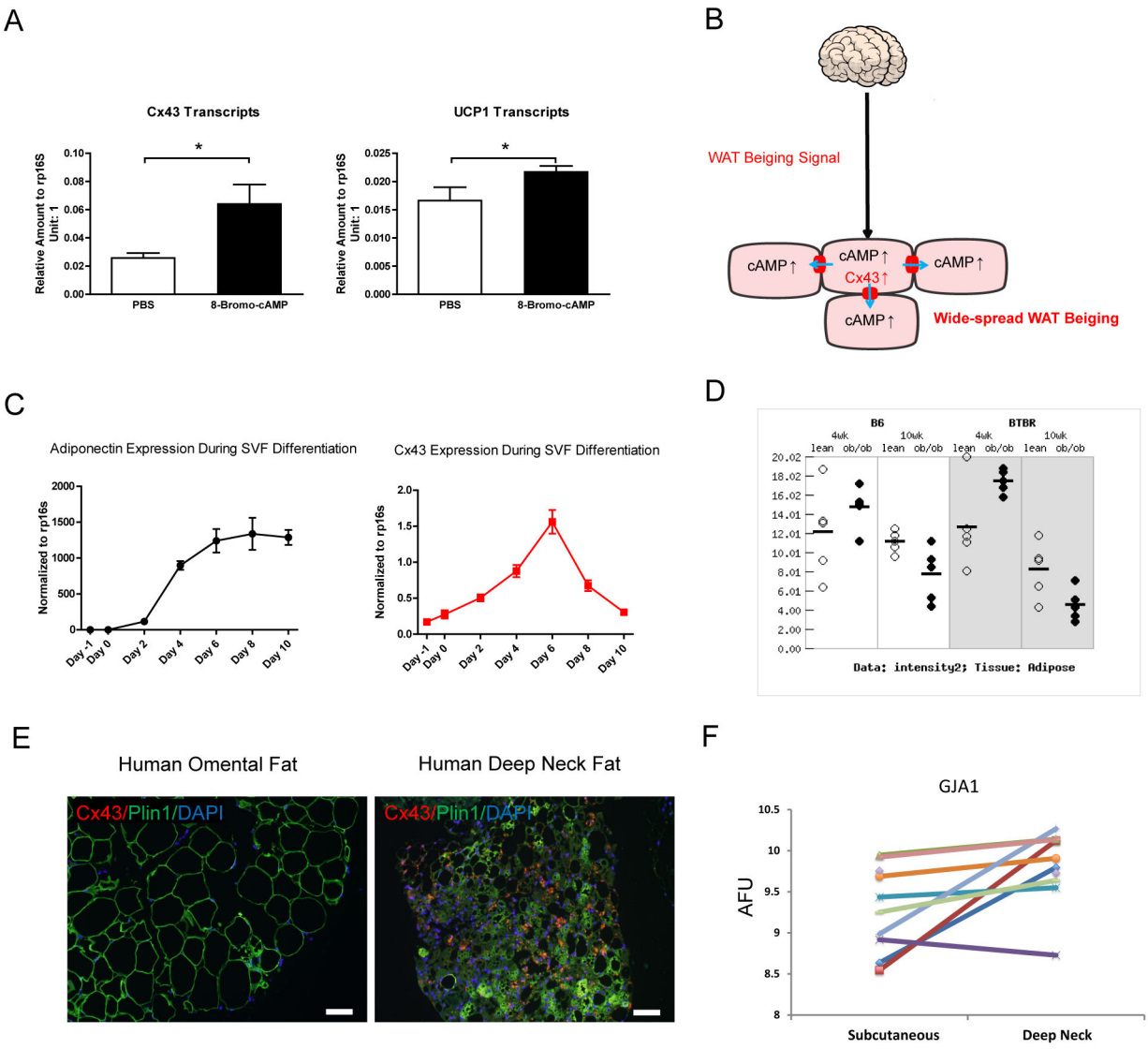

Figure 7. A Working Model for the Cx43-Mediated Propagation of WAT Beiging Signals and the Clinical Implications of these Observations

A. Cx43 and UCP1 expression after 8-Bromo-cAMP treatment in differentiated mouse adipocytes (n = 8). **B.** A working model of how sympathetic neuronal signal increases Cx43 expression to allow cAMP diffusion to adjacent adipocytes to spread the signal and reach a widespread WAT beiging. **C.** Cx43 expression levels decreased during the *in vitro* cultured mouse primary adipocyte late-stage differentiation and lipid droplets accumulation (n = 4). **D.** Expression of Cx43 in adipose tissue from *ob/ob* mice on both B6 and BTBR genetic backgrounds at two different ages (derived from the Alan Attie Diabetes Database, http://diabetes.wisc.edu/). **E.** Human deep neck fat (beige/brown adipose) showed high levels of Cx43 immunofluorescent staining in comparison to the absence of Cx43 signals in human omental fat. **F.** Gene expression analysis of GJA1 (encoding human Cx43 protein) between human deep neck fat and subcutaneous fat showed higher GJA1 expression in the human

deep neck fat ($p = 0.011$, $n = 10$). Scale bar = 100 μm. Results are shown as mean ± SEM, *$p<0.05$.